CHEMISTRY OF HIGH TEMPERATURE SUPERCONDUCTORS

Edited by
C. N. R. RAO, *F.R.S.*
CSIR Centre of Excellence in Chemistry and Solid State and Structural Chemistry Unit
Indian Institute of Science, Bangalore, India

World Scientific
Singapore • New Jersey • London • Hong Kong

Published by

World Scientific Publishing Co. Pte. Ltd.
P O Box 128, Farrer Road, Singapore 9128
USA office: Suite 1B, 1060 Main Street, River Edge, NJ 07661
UK office: 73 Lynton Mead, Totteridge, London N20 8DH

Library of Congress Cataloging-in-Publication Data

Chemistry of high-temperature: superconductors/edited by C.N.R. Rao.
p. cm.
Includes bibliographical references.
ISBN 9810208057
1. High temperature superconductors. 2. Superconductivity-Chemistry. 3. Solid state chemistry. I. Rao, C. N. R. (Chintamani Nagesa Ramachandra), 1934-
QC611.98.H54C47 1991
527.6'23--dc20 91-32649
CIP

Printed in Singapore by Utopia Press.

CHEMISTRY OF HIGH TEMPERATURE SUPERCONDUCTORS

PREFACE

Superconductivity has become one of the most active areas of research in physical sciences in the last few years, because of the advent of high-temperature superconductivity in oxide materials, especially the cuprates. Since the initial discovery of 30 K superconductivity in the La-Ba-Cu-O system by Bednorz and Müller, a variety of materials with novel structural features have been synthesized and characterized. Several interesting correlations between the structure and the properties of superconducting oxide materials have been unravelled. While most cuprate superconductors have holes as charge carriers, electron superconducting cuprates have also been discovered. There are also a few oxide superconductors which do not have copper in them. In all these developments, chemists have made many important contributions. In this volume an effort has been made to present the status of the chemistry of high-temperature oxide superconductors. It is possible that certain aspects such as crystal growth and measurements on single crystals have not been adequately covered in this volume. However, the various articles presented here should cover most of the salient features of high-temperature oxide superconductors with respect to synthesis, structure, and properties. Wherever possible preparative aspects are highlighted and two review articles deal with thin films besides one article with tapes. I believe that by going through the articles in this volume, one will be able to get a nearly complete picture of the present status of the chemical aspects of high-temperature oxide superconductors, with a useful set of references to most of the recent literature. It is hoped that some of the ideas mentioned in these articles would also stimulate further research.

High-temperature superconductivity itself is going through an interesting phase today. Newer materials are likely to be discovered in the near future. We already have the alkali metal doped buckminsterfullerene, C_{60}, showing superconductivity around 40 K.

I do hope that the present volume will be found useful by students, teachers, and practitioners.

C.N.R. RAO
Bangalore
July 1991

CONTENTS

CRYSTAL CHEMISTRY AND SUPERCONDUCTIVITY IN THE COPPER OXIDES

J. B. GOODENOUGH and A. MANTHIRAM
Center for Materials Science and Engineering, ETC 5.160
University of Texas at Austin
Austin, Texas 78712-1084

ABSTRACT

This article highlights the importance of crystal chemistry in controlling the superconductive properties of the copper oxides. Stabilization of their intergrowth structures requires bond-length matching across the intergrowth interface. At least four different structures -- T/O, T ', T* and T " -- are stabilized in the simplest system $La_{2-y}Ln_yCuO_4$ (Ln = lanthanide) depending upon the size of the Ln atom and the value of y. Whether the CuO_2^{2-} sheets of a parent intergrowth structure can be oxidized or reduced to give p-type or n-type superconductors is determined by the basal plane Cu-O distances as well as the oxygen coordination number around the Cu atoms. The internal electric field created by the formal charges in the adjacent layers as well as the preferred oxidation states for different coordination geometries around Cu appear to modulate the distribution of holes between active and inactive layers, *e.g.* in $YBa_2Cu_3O_{6+x}$. Realization of superconductivity requires the maintenance of a uniform periodic potential -- *i.e.* a uniform oxygen coordination -- around the Cu atoms. Although the overlap of a localized $4f^n$ level by the conduction band suppresses superconductivity, as in $Y_{1-z}Pr_zBa_2Cu_3O_{6+x}$, overlap of a Tl-6s band does not. A thorough investigation of the chemistry-structure-property relationships for the simplest system $La_{2-y}Sr_yCuO_4$ has led to the identification of the charge fluctuations that separate antiferromagnetic-spin fluctuations from superconductive regions as a result of strong electron-phonon interactions in these materials.

1. Crystal Architecture

With one exception, the known copper-oxide superconductors all crystallize with intergrowth structures consisting of superconductive oxide layers alternating with nonsuperconductive oxide layers. The exception consists of a superconductive layer of infinite width. The superconductive layers have a fixed oxygen content and contain one or more CuO_2 planes (or sheets if the planes are buckled) with *ca.* 180 ° Cu-O-Cu bonds. The nonsuperconductive oxide layers may have a variable oxygen content.

Oxidation/reduction of the CuO_2 sheets above/below the formal oxidation state $(CuO_2)^{2-}$ — but maintaining the same oxygen coordination at all the copper atoms of a sheet — is a necessary condition to induce superconductivity. All the copper-oxide superconductors have parent structures with antiferromagnetic $(CuO_2)^{2-}$ sheets; the superconductors have a mixed valence in the CuO_2 sheets. Oxidation of the CuO_2 sheets gives p-type superconductivity; reduction of the CuO_2 sheets gives n-type superconductivity. Whether the $(CuO_2)^{2-}$ sheet of an antiferromagnetic parent compound can be oxidized or reduced sufficiently to become superconductive appears to be controlled

principally by the Cu-O bond length and the oxygen coordination number of the copper atoms, both of which are strongly influenced by the non-superconductive intergrowth that stabilizes the parent structure.

The p-type intergrowth superconductors have nonsuperconductive layers bounded by rocksalt AO (A = Ba, Sr or La) sheets that interface with an active CuO_2 sheet of the adjacent superconductive layer. The n-type superconductors have superconductive CuO_2 planes that interface on each side with planes of cations stable in eightfold coordination. Hybrid intergrowths having two different types of nonsuperconductive layers are also known; in a hybrid the superconductive layer is interfaced on one side by an AO rocksalt layer adjacent to a CuO_2 sheet and on the other by a cation plane adjacent to a CuO_2 sheet. These three situations are illustrated by the simplest parent structures of formula Ln_2CuO_4 shown in Fig. 1; they are contrasted with the parent structure $Sr_{0.14}Ca_{0.86}CuO_2$ shown in Fig. 2, which has no nonsuperconductive oxide intergrowth.

This basic structural architecture has four important consequences:

(1) Oxidation/reduction of the CuO_2 sheets/planes of a superconductive layer may be achieved without changing the CuO_2 sheets or the oxygen coordination of the copper in the superconductive layers by either (a) aliovalent cation substitution for a non-copper cation or (b) aliovalent-anion substitution or anion insertion/extraction within a nonsuperconductive layer.

(2) Strong electronic and elastic anisotropy complicates the fabrication of useful devices; it also tends to remove the orbital degeneracy of the partially occupied conduction band.

(3) The requirement of bond-length matching across an intergrowth interface introduces internal strains relative to the normal equilibrium bond lengths.

(4) Opposite formal charges on the intergrowth layers introduce internal electric fields that shift the energies of adjacent layers relative to one another.

In Section 2, we illustrate the role of bond-length matching in the determination of the phase relationships with the simplest of the intergrowth structures. We also review some of the complex intergrowth structures that have been synthesized.

In Section 3, we discuss how the energies of the Cu(II/I) and Cu(III/II) redox potentials are determined by the internal electric fields and how, in an intergrowth structure, these fields are influenced by (a) the oxygen coordination at a copper atom, (b) the mean Cu-O bond length, and (c) the formal charges on the intergrowth layers.

Section 4 reviews the phase diagram for the system $La_{2-y}Sr_yCuO_4$ as illustrative of the evolution in properties that occur on passing from an antiferromagnetic parent compound through a superconductive phase to a normal metallic state with increasing oxidation/reduction of the CuO_2 sheets/planes of a superconductive layer. A change from more ionic to more covalent Cu-O bonding is emphasized. This discussion leads to a review of the "correlation bag" model of superconductivity (section 5), which appears to survive as a possible mechanism for the high-T_c superconductivity found in these oxides.

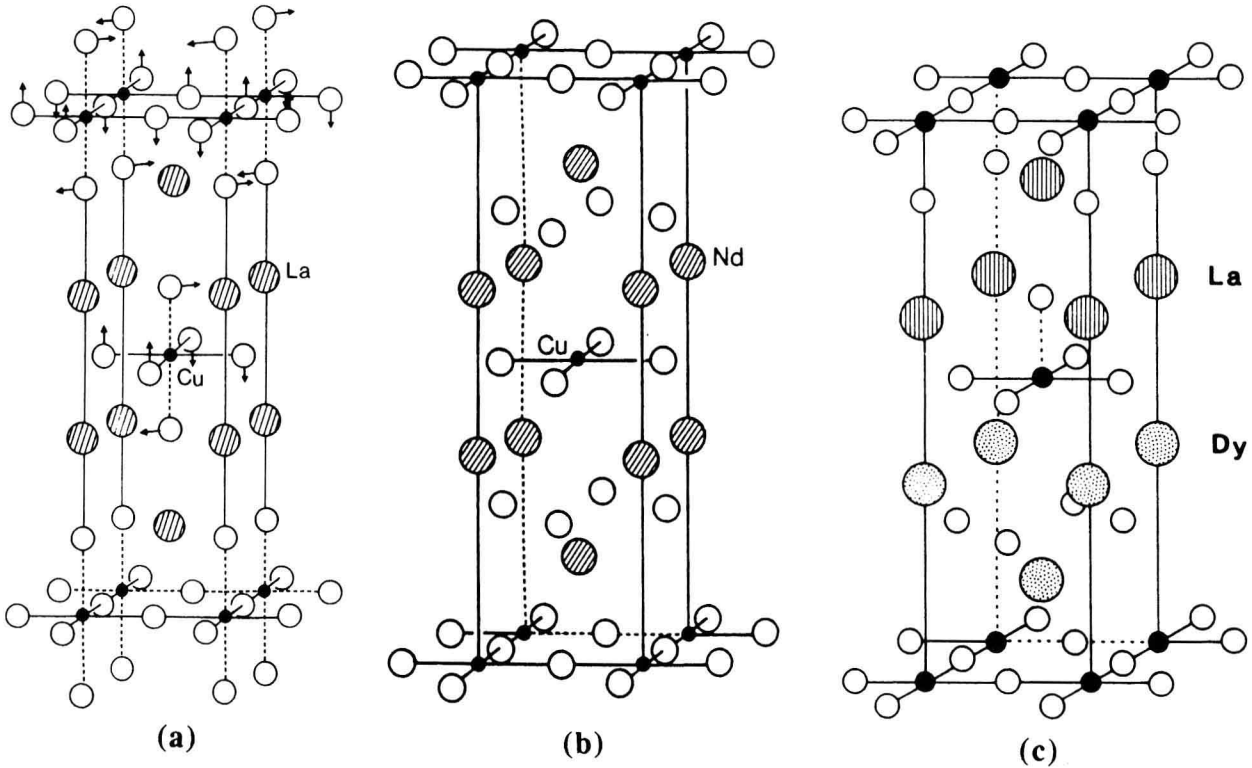

Fig. 1. Structures of (a) T/O-La_2CuO_4, (b) T'-Nd_2CuO_4 and (c) T^*-$LaDyCuO_4$.

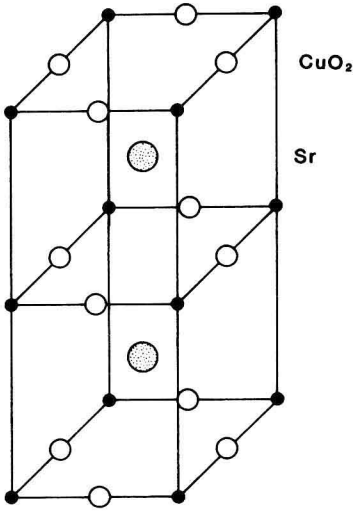

Fig. 2. Structure of the infinite-layer compound $SrCuO_2$.

2. Bond-length Matching

2.1 The Tolerance Factor for the Ln_2CuO_4 Compounds

The parent compound La_2CuO_4 of Fig. 1(a) is an antiferromagnetic insulator [1]. At high temperatures it is tetragonal; below a transition temperature $T_t \approx 500$ K, a cooperative rotation, see arrows in Fig. 1(a), of the CuO_6 octahedra about [110] axes in the CuO_2 planes distorts the structure to orthorhombic symmetry and buckles the CuO_2 planes into CuO_2 sheets[2]. In the tetragonal phase, a single CuO_2 plane is bounded on either side by (001) LaO rocksalt planes; we represent this T/O-tetragonal/orthorhombic phase schematically as

$$\ldots \text{LaO}|\text{CuO}_2|\text{LaO-LaO}|\text{CuO}_2|\text{LaO} \ldots \qquad (1)$$

where the vertical lines separate the intergrowth layers consisting, in this case, of a single CuO_2 plane and a double rocksalt layer. A measure of the bond-length mismatch across the interfaces represented by the vertical lines is the *tolerance factor*

$$t \equiv (\text{A-O})/\sqrt{2}\,(\text{B-O}) \qquad (2)$$

where, for La_2CuO_4, A-O and B-O are the equilibrium La-O and Cu-O bond lengths at any given temperature T and pressure P. From Fig. 1(a), a t = 1 corresponds to a perfect bond-length matching.

Historically, Goldschmidt defined a tolerance factor

$$t = (r_A + r_O)/\sqrt{2}\,(r_B + r_O) \qquad (3)$$

for the ABO_3 perovskite; r_A, r_B and r_O are the empirically determined ionic radii developed from room-temperature x-ray data at ambient pressure. This definition proved useful for classifying the range of t about t = 1 in which the perovskite structure is stable relative to competitive structures such as ilmenite or the hexagonal perovskite polytypes [3]. However, the more general formulation (Eq. 2) is to be preferred as it allows for the different compressibilities and thermal-expansion coefficients of the A-O and B-O bond lengths that cause it to depend on temperature and pressure.

In the Ln_2CuO_4 compounds, the Ln-O bond is softer than the in-plane Cu-O bond, which makes $dt/dT > 0$ and $dt/dP < 0$. Moreover a $t < 1$ places the Cu-O planes of the T-tetragonal phase under compression and the Ln-O bonds under tension. This bond-length mismatch increases with decreasing temperature, and it is of interest to see how nature adjusts to the mismatch . In the case of La_2CuO_4, which has a Goldschmidt factor $t = 0.89 < 1$ as calculated from the Shannon[4] empirical ionic radii, three distinct adjustments can be identified.

(1) The single hole in the 3d shell of a Cu(II) ion is ordered into orbitals of x^2-y^2 symmetry; these σ-bond within the CuO_2 planes, and the partially occupied antibonding orbitals of x^2-y^2 symmetry are referred to as $\sigma^*_{x^2-y^2}$ orbitals. This removal of the e_g-orbital degeneracy of the octahedral-site Cu(II):$3d^9$ configuration is reflected in a large tetragonal ($c/a > 1$) distortion of the CuO_6 octahedra [2]. The in-plane Cu-O distances are 1.91 Å and the apical Cu-O distances are 2.46 Å.

(2) On slow cooling in 1 atm air from a synthesis temperature of 1000 °C, interstitial oxygen are inserted between the two LaO planes of a rocksalt layer

$$\ldots LaO|CuO_2|LaO\text{-}O_\delta\text{-}LaO|CuO_2|LaO\ldots \qquad (4)$$

to create an oxygen-rich composition $La_2CuO_{4+\delta}$. The interstitial oxygen atoms occupy sites coordinated by four La^{3+} and four apical O^{2-} ions. Each interstitial oxygen captures two electrons form the CuO_2 sheets. Removal of antibonding $\sigma^*_{x^2-y^2}$ electrons from the CuO_2 sheets relieves the compressive stress on the sheets, and an electrostatic repulsion between the interstitial oxide ions and their four neighboring apical O^{2-} ions relieves the tension in the rocksalt layers. However, at atmospheric pressure the solid-solubility range for the interstitial oxide ions is restricted. Moreover, preparations under high oxygen pressure[5,6] have revealed the existence of distinguishable antiferromagnetic and superconductive phases below room temperature with, from neutron-diffraction data[7], a two-phase compositional range $0.02 < \delta < 0.08$. Slow cooling in air commonly gives a *filamentary superconductivity* associated with an oxygen-rich surface layer; however, a poor kinetics for oxygen insertion at oxygen partial pressures ≤ 1 atm does not permit insertion of enough interstitial oxygen for bulk superconductivity. In the absence of high

oxygen pressures, the relief of the internal stresses by the insertion of interstitial oxygen is therefore limited, so a third adjustment comes into play at lower temperatures.

(3) Since $t < 1$ continues to decrease with decreasing temperature where further oxygen insertion is kinetically blocked, the internal stresses are relieved by a distortion form tetragonal to orthorhombic symmetry below $T_t \approx 500$ K. We therefore refer to La_2CuO_4 as having a T/O structure. Below T_t, the compressive stress in the CuO_2 planes is relieved by a buckling of the Cu-O-Cu bonds within the CuO_2 sheets from 180 ° and the tension in the rocksalt layers is relieved by a reduction of some of the La-O bond lengths.

It follows from the above analysis that the orthorhombic-tetragonal transition temperature T_t must decrease with increasing δ in $La_2CuO_{4+\delta}$, $\delta \leq 0.02$, and also with y in $La_{2-y}Sr_yCuO_4$ since the Sr^{2+} ion is larger than the La^{3+} ion and its substitution for a La^{3+} ion oxidizes the CuO_2 sheets. However, at higher concentrations δ of interstitial oxygen, an alternative orthorhombic distortion arises from interactions between the local elastic strains around an interstitial atom. This orthorhombic phase has a T/O transition temperature that increases with δ.

On the other hand, if a Ln = Pr - Gd rare-earth atom is used instead of the larger La^{3+} ion in Ln_2CuO_4, then the internal stresses associated with a $t < 1$ become too large even at the synthesis temperature to retain the T/ O structure of Fig. 1(a). In this case, the internal stresses are relieved by a fourth mechanism.

(4) The apical oxygen atoms of Fig. 1(a) are displaced to the interstitial-oxygen sites; this displacement transforms the (001) LnO-LnO rocksalt bilayer into an (001)Ln-O_2-Ln fluorite layer[8], see Fig. 1(b), and leaves the copper in square-coplanar coordination within CuO_2 planes. The parent compound Nd_2CuO_4, for example, has this T ' tetragonal structure with 180 ° Cu-O-Cu bonds over the entire temperature range 4 - 1200 K [9]. For the larger Pr^{3+} and Nd^{3+} ions, the fluorite layers are under compression and the CuO_2 planes are under tension. However, as the size of the Ln^{3+} ion is reduced from Pr^{3+} to Gd^{3+}, the Cu-O bond length within the CuO_2 planes decreases, which relieves the tension in the plane. It is necessary to use high pressure[10] to synthesize Ln_2CuO_4 compounds with the T '-tetragonal structure where the Ln^{3+} ion is smaller than Gd^{3+}; in these high-pressure phases, the CuO_2 planes may be under a residual compressive stress that could buckle the 180 ° Cu-O-Cu bonds at lower temperature.

Nd_2CuO_4 is an antiferromagnetic insulator with an ambient-temperature Cu-O bond length of 1.97 Å[8]; we represent its T '-tetragonal structure schematically as

$$\ldots \text{Nd}|\text{CuO}_2|\text{Nd-O}_2\text{-Nd}|\text{CuO}_2|\text{Nd} \ldots \qquad (5)$$

in which, ideally, the CuO_2 planes are interfaced on either side by Nd planes.

The hybrid parent structure of Fig. 1(c), designated as T *-tetragonal, is found where two different lanthanide ions of significantly different size are used as in

$La_{2-y}Ln_yCuO_4$, $0.75 \lesssim y \lesssim 1.0$ and Ln = Sm-Dy [11-15]. This tetragonal structure has a layer sequence along the *c*-axis given ideally by

$$\ldots CuO_2|LaO\text{-}LaO|CuO_2|Ln\text{-}O_2\text{-}Ln|CuO_2 \qquad (6)$$

in which the larger La^{3+} and the smaller Ln^{3+} ions are preferentially ordered, respectively, into the rocksalt and fluorite layers. Only the Ln^{3+} ions Sm^{3+} and smaller can form a fluorite layer that has an *a*-parameter small enough to be compatible with that of a LaO-LaO rocksalt layer. The interplanar ordering of the La^{3+} and Ln^{3+} ions has been confirmed by neutron diffraction [11,15,16]. The T *-tetragonal phases have a unit-cell *a*-parameter intermediate to those of the T/O and T ' phases, and the copper of the CuO_2 sheets have fivefold oxygen coordination. Moreover, the symmetry allows a bending of the Cu-O-Cu bonds from 180 °, so there is no distortion from tetragonal symmetry on cooling.

2.2. Phase Relationships in $La_{2-y}Nd_yCuO_4$

Partial substitution of the larger La^{3+} ions by Ln = Pr^{3+} or Nd^{3+} ions does not give the T *-tetragonal structure; the larger sizes of the Nd^{3+} and Pr^{3+} ions are not compatible with a LaO-LaO rocksalt intergrowth coexisting with, for example, a Nd-O_2-Nd fluorite layer. Nevertheless, the systems $La_{2-y}Ln_yCuO_4$, Ln = Pr or Nd, give interesting phase relationships that not only demonstrate the control of the T/O versus T ' structure by the bond-length mismatch across the $LnO|CuO_2$ interface, but also the temperature dependence of the tolerance factor t [17-19].

Fig. 3 shows the variation of the room-temperature lattice parameters versus composition y for the system $La_{2-y}Nd_yCuO_4$ obtained by firing the component oxides at 1050 °C followed by annealing at 400 °C in 1 atm O_2. Also shown is the compositional dependence of the Goldschmidt tolerance factor of Eq. 3. The T/O structure of Fig. 1(a) is found for $0 \leq y \leq 0.35$ and $t \geq 0.866$; the T ' structure of Fig. 1(b) for $1.2 \lesssim y \leq 2.0$ and $t \lesssim 0.859$. The phase boundaries between the T/O and T ' phases occur at similar values of the Goldschmidt tolerance factor for the $La_{2-y}Pr_yCuO_4$ system. In addition, in both systems a new line phase — designated as T " — appears at y = 0.5; it has an x-ray pattern like that of the T ' phase, and neutron-diffraction data[20] show an oxygen ordering like that of the T ' phase. Although Bringley *et al* [21,22] did not distinguish it from the T ' phase, several indirect experiments have shown it to be a distinct phase[17-19]. For example, the intermediate compositional range $0.55 < y < 1.2$ consists of two phases, T ' and T "; no evidence for a T * phase was found near y = 1.0. The T " phase appearing instead at a La:Ln ratio 3:1 for both the Pr and Nd systems suggests that the interplanar ordering of the T * phase is replaced by an intraplanar cation ordering within the fluorite layers. Although long-range interplanar cation ordering has not been observed by neutron diffraction [20], extensive short-range ordering within the $La_{1.5}Ln_{0.5}O_2$ fluorite layers would lower the net energy of the T ' structure; we believe such an ordering stabilizes the T " phase relative to the T/O phase. This hypothesis can be checked with XAFS.

We also investigated the phase relationships in $La_{2-y}Nd_yCuO_4$ as a function of the synthesis temperature — Fig. 4 — by firing the copreciated hydroxides/carbonates at 500 -

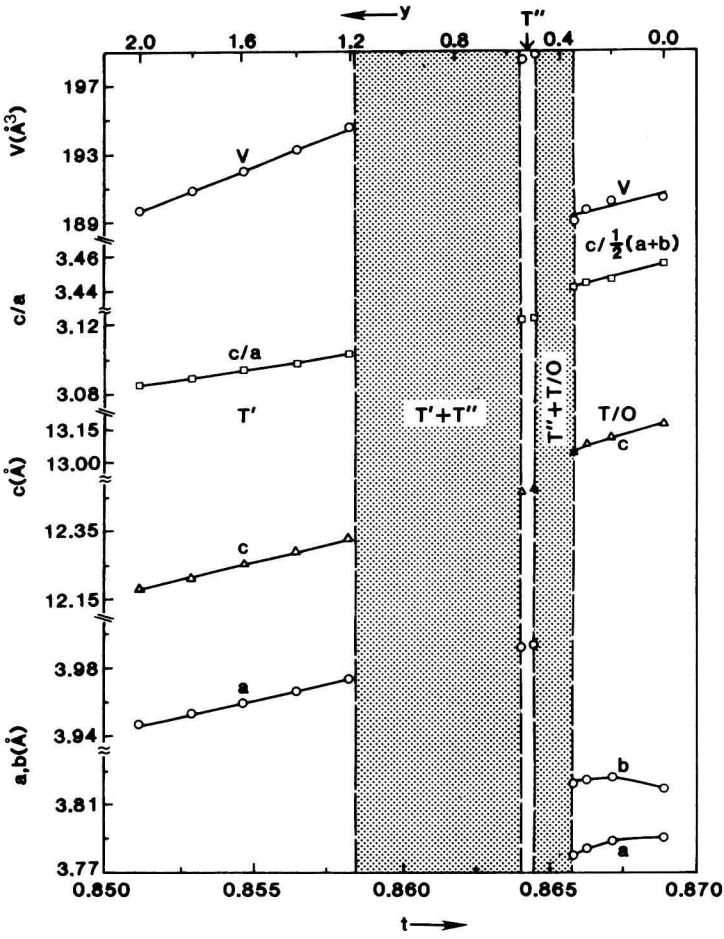

Fig. 3. Variation of room-temperature lattice parameters and volume with t or y for the system $La_{2-y}Nd_yCuO_4$; t values were obtained with the nine-coordinated Shannon radius for La^{3+} and Nd^{3+} for all values of y. For comparison, the *a* and *b* parameters for the T/O phases are plotted after dividing the actual orthorhombic parameter by $\sqrt{2}$.

1050 °C [19]. The range of the T/O phase field is seen to increase progressively to higher Nd concentration as the synthesis temperature is increased. This finding provides a direct confirmation of the increase in tolerance factor t with temperature T; if there were no difference in the thermal expansions of the equilibrium Ln-O and Cu-O bond lengths, the phase boundary would be expected to occur at the same value of the Goldschmidt factor —

Eq. 3 — for all synthesis temperatures. Moreover, extrapolation of the data of Fig. 4 to lower temperatures indicates that La_2CuO_4 can be stabilized in the T ' structure if the synthesis is carried out below 425 °C. Although we obtained a T/O + T ' two-phase mixture for La_2CuO_4 synthesized at 500 °C, we could not obtain single-phase T ' La_2CuO_4 as our synthetic procedure required firing temperatures $T \gtrsim 500$ °C. However, Chou *et al.*[23] have obtained T '-La_2CuO_4 by reducing T/O La_2CuO_4 with hydrogen around 300 °C followed by reoxygenation below 400 °C.

Below 850 °C, the T/O + T ' two-phase region in Fig. 4 has a constant width of $\Delta y \approx 0.2$; for synthesis temperatures T > 850 °C, the phase relationship is complicated by the appearance of the T " phase at $y \approx 0.5$ within the T/O phase field. A higher synthetic

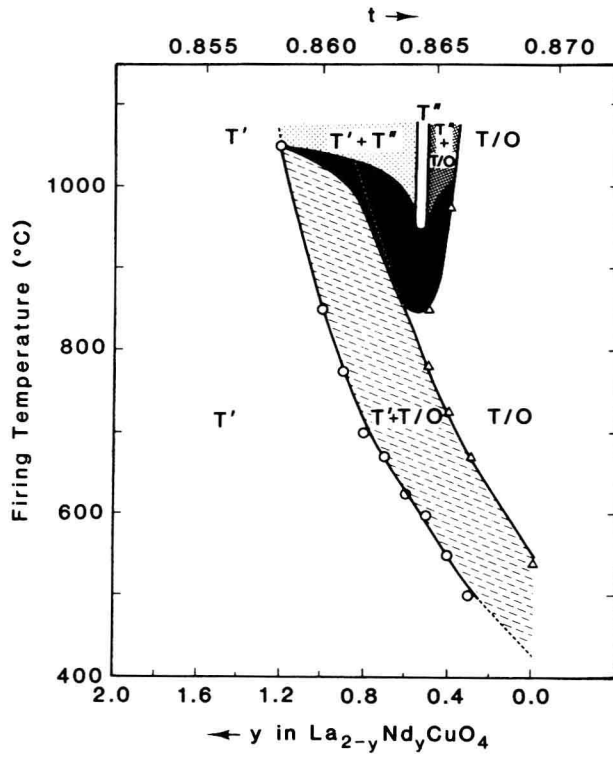

Fig. 4. Phase relationships for the system $La_{2-y}Nd_yCuO_4$ obtained by firing the coprecipitated hydroxides/carbonates progressively at higher temperatures followed by cooling to room temperature. The thickly shaded area around 850 - 1050 °C and $y \approx 0.5$ represent a non-equilibrated region consisting of T/O, T ' and T " phases.

temperature provides a higher cation mobility and hence the possibility of cation ordering within a fluorite layer of the T ' structure. Sufficient cation mobility above 950 °C allows realization of the equilibrium phase diagram around $y \approx 0.5$. The thickly shaded region from 850-1050 °C near $y \approx 0.5$ represents a nonequilibrated domain in which T ', T/O and T " phases are all found.

The phase relationships of Fig. 4 can be modified by changing the oxygen concentration. For example, Bringley *et al.*[22] have stabilized T/O-$La_{1.4}Nd_{0.6}CuO_{4.04}$ by firing the copreciated hydroxides at 910 °C and 400 bar O_2 as well a T "-$La_{1.4}Nd_{0.6}CuO_{3.98}$ (identified by them as T ') by annealing at 1050 °C in air followed by quenching. The insertion of interstitial oxygen into the T/O phase is equivalent to increasing t — see the discussion above — and the $y \approx 0.6$ composition lies close to the T/O phase boundary at 850 °C, see Fig. 4. Therefore, the insertion of interstitial oxygen shifts the T/O phase boundary sufficiently to stabilize T/O-$La_{1.4}Nd_{0.6}CuO_{4.04}$ synthesized at 910 °C. For relatively short firing times at 900 °C, there would be no formation of the T " phase, which needs sufficient cation mobility and time for equilibration. However, at 1050 °C the T " phase would be rapidly formed in the absence of excess oxygen.

Attempts to dope the T " phase either n-type or p-type by substitutions of Ce^{4+} or Sr^{2+} for either La^{3+} or Nd^{3+} were unsuccessful. Ce^{4+} substitutions resulted in a disproportionation into an n-type T ' phase and an undoped T/O phase; Sr^{2+} substitution resulted in a disproportionation into p-type T/O and undoped T ' phases[17,19]. These two situations are illustrated in Fig. 5. The observation that cation substitutions in the inactive layer result in a simple phase diagram — Fig. 5(b) — containing only T ' and T/O phase fields supports the hypothesis that the T " phase is stabilized by a cation ordering within the inactive layers.

2.3. Complex Intergrowths and Bond-Length Matching

Figs. 6-9 illustrate some of the more complex copper-oxide intergrowth structures that exhibit high-T_c superconductivity. The system $YBa_2Cu_3O_{6+x}$ of Fig. 6 [24] may be represented as

$$\ldots CuO_2|BaO\text{-}CuO_x\text{-}BaO|CuO_2\text{-}Y\text{-}CuO_2|BaO\ldots \qquad (7)$$

in which the nonsuperconductive layer BaO-CuO_x-BaO also contains copper and has a variable oxygen content $0 \le x < 1$. With two CuO_2 sheets per superconductive layer and a rocksalt BaO layer at the interface, the copper of the superconductive CuO_2 sheets have fivefold oxygen coordination with Cu-O-Cu bond angles bent from 180 °. The structure also allows the *c*-axis (apical) oxygen O(1) freedom to move along the *c*-axis, which means that the Ba-O-Ba bonds are bent from 180 °. Ordering of the oxygen within the CuO_x plane for $0.45 < x < 1$ along a unique Cu-O-Cu bond axis transforms the symmetry from tetragonal to orthorhombic, and the resulting compression along this *b*-axis is relieved by a cooperative rotation about the *c*-axis of the square-coplanar coordination about the Cu(1) atoms of a CuO_x plane; this cooperative rotation bends the Cu-O-Cu bonds from 180 ° in this plane also.